ANALYSIS OF SEISMIC RESPONSE OF SEVEN OAKS DAM

Lelio H. Mejia and Ethan M. Dawson

URS Corporation
Oakland, California

Abstract

Procedures for the three-dimensional (3-D) dynamic analysis of earth dams have been available for over 25 years. However, additional case histories are needed to assess whether such procedures are capable of simulating the seismic response of dams in narrow canyons, and to further evaluate the effects of 3-D behavior on the response of such dams. This paper describes a study aimed at identifying the vibration characteristics of Seven Oaks Dam during the 2005 Yucaipa and 2001 Big Bear Lake earthquakes, and at evaluating the applicability of 3-D and two-dimensional numerical procedures to simulate the recorded response of the dam.

Introduction

The seismic stability evaluation of earth and rockfill dams typically requires an analysis of their dynamic response to earthquake shaking. Such analysis is commonly performed using finite element procedures. Although procedures for the three-dimensional (3-D) dynamic response analysis of earth dams in narrow canyons have been available for over 25 years, they are seldom used in practice for design purposes. This is mainly because: a) the effects of 3-D behavior on the seismic stability of such dams are generally believed to be beneficial, and b) the modeling and computational effort associated with 3-D analysis is significantly greater than that associated with two-dimensional (2-D) analysis.

Previous studies have shown that 3-D behavior can have a pronounced effect on the seismic response of earth dams with crest length to height ratios less than about 6 (e.g. Boulanger et al., 1995, Dakoulas, 1993, Mejia and Seed, 1983). Three-dimensional behavior of such dams can result in significantly larger accelerations at the dam crest than might otherwise be expected based on 2-D analysis procedures. Thus, for such types of dams, 3-D analysis procedures may be required to adequately evaluate their acceleration response and potential for seismic deformations.

Additional case histories of dams in narrow canyons are needed to: a) assess the effects of 3-D behavior on the seismic response of those types of dams and the extent to which available methods of 3-D analysis adequately simulate their response, and b) develop guidance for the use of 3-D analysis methods in engineering practice. One such case history is the recorded seismic response of Seven Oaks Dam during the June 16, 2005 Yucaipa and the February 10, 2001 Big Bear Lake earthquakes.

This paper describes a study aimed at identifying the modes of vibration of Seven Oaks Dam during the aforementioned earthquakes and evaluating the applicability of 3-D and 2-D numerical models to simulate the recorded dynamic response of the dam. Because the dam has a curved axis and sits in a canyon of limited width, it may be expected to exhibit 3-D behavior under earthquake shaking. Thus, given that the dam site is well instrumented with strong motion accelerographs, this case history offers an excellent opportunity to evaluate the effects of 3-D vibration modes on the seismic response of a large dam in a relatively narrow canyon, and the ability of available 3-D and 2-D numerical techniques to simulate the key aspects of the dam's recorded response.

Description of Seven Oaks Dam

General

Seven Oaks Dam is a zoned rockfill embankment located on the Santa Ana River about 10 km northeast of the city of Redlands in San Bernardino County, California. The dam was completed in 1999 by the U.S. Army Corps of Engineers (USACE) primarily to provide downstream flood protection to Orange County and other areas of the Santa Ana River Basin. The site is located about 2 km from the San Andreas Fault, and the dam was designed to withstand a maximum credible earthquake of magnitude 8+ on that fault (USACE, 1992; Makdisi et. al, 1996).

The dam has a structural height of about 640 feet, a crest length of 2,760 feet, and a volume of 38 million cubic yards. As shown in Figure 1, the embankment is curved upstream and its width is approximately equal to its length. The outlet works are located on the left abutment and consist of an intake tower, an 18-foot-diameter tunnel, an outlet channel, and a plunge pool. A vertical shaft provides air supply and access to a gate chamber located just downstream of the tunnel midpoint (Figure 1). The spillway is a 500-foot-wide channel cut through a rock ridge east of the left abutment, with a crest elevation 30 feet below that of the dam crest.

Embankment and Foundation Materials

Figure 2 shows the maximum section of the dam, which is located near the midpoint of the crest. The embankment consists of a moderately inclined upstream sloping core flanked upstream by a filter, and alluvial transition and shell zones. On the downstream side, the core is supported by a rockfill transition zone, a chimney drain, and a rockfill shell. A blanket drain extends from the base of the chimney drain beneath the downstream rockfill shell. Along the stream bed, the upstream and downstream shells are founded on very dense alluvium in turn underlain by bedrock. The core is directly founded on bedrock in a trench excavated through the alluvium.

The dam materials were placed to modern compaction standards and may be considered as generally very dense. The core consists of clayey and silty sands with over 25% fines of low to medium plasticity. The filter and drains are sands and gravels processed from alluvial materials. The alluvial transition consists of processed minus 12-inch cobbles, gravels, and

sands and the alluvial shell of minus 18- to 30-inch cobbles and boulders. The rock transition and rockfill materials are sand to minus 9-inch and 15-inch boulders, respectively, processed from the spillway and other rock excavations.

Because the alluvial transition and shell materials are expected to exhibit similar dynamic behavior, those two zones, together with the upstream filter, were combined into a single zone (designated herein as alluvial fill) for purposes of dynamic analysis. Likewise, the rockfill transition, downstream filter and drain, and rockfill shell were combined into a single zone (designated as rockfill).

Material Properties

For dynamic response analysis of the dam, the key material properties are the dynamic shear modulus at small strain, G_{max}, the unit weight of the materials, γ, Poisson's ratio, ν, and the relationships between normalized shear modulus, G/G_{max}, and damping ratio with shear strain. The maximum shear modulus may be obtained from the shear wave velocity of the materials, V_s, by the following expression: $G_{max} = V_s^2\gamma/g$, where g is the gravitational constant. For granular soils, the maximum shear modulus may be expressed as a function of the mean effective stress, σ_m', as follows: $G_{max} = K_{2max}(\sigma_m')^{1/2}$, where K_{2max} is a constant, σ_m' is in psf and G_{max} is in ksf.

Extensive field and laboratory tests were carried out prior to construction to characterize the embankment and foundation materials (USACE, 1992). The laboratory tests included cyclic triaxial and resonant column tests of the core materials and of scaled-down gradations of the transition materials. Field tests included multiple seismic refraction surveys in the foundation alluvium and rock, and in compaction test fills. Crosshole and downhole surveys were also used to measure the shear and compression wave velocities of compacted alluvial and rockfill materials in the test fills, and of the underlying foundation alluvium. However, no measurements of the shear and compression wave velocities of the dam materials in place are available.

Table 1 summarizes the key material properties selected for initial dynamic analysis of the dam from examination of the available data. The values of K_{2max} for the alluvial fill, the rockfill, and the foundation alluvium were obtained from the crosshole velocity measurements in the test fills. The K_{2max} value obtained by the USACE (1992) from the dynamic laboratory tests on the core materials was adopted for the core. The rock shear wave velocities were synthesized from the seismic refraction data.

Limited information is available on the modulus reduction and damping relationships of coarse alluvial fill and rockfill. Previous studies of the seismic response of rockfill dams have made the assumption that such relationships may be approximated by available relationships for cohesionless soils. Boulanger et al. (1995) and Mejia et al. (1991) showed that use of the relationships proposed by Seed et al. (1986) for gravels provided a reasonable approximation to the recorded response of two rockfill dams. Rollins et al. (1998) compiled modulus reduction and damping data for sandy gravels and gravelly sands, which fell over the range defined by the relationships by Seed et al. (1986) for gravels and those proposed for sands by Seed and Idriss (1970). Hardin and Kalinski (2005) presented modulus reduction data for gravels and gravelly sands, which appear to be well represented by the Seed et al. gravel relationship. They also

showed that the relationship between normalized modulus, G/G_{max}, and shear strain normalized by the ratio $(\sigma_m'/P_a)^{1/2}$, where P_a is atmospheric pressure, is independent of effective stress.

On the above basis, the Seed et al. (1986) gravel relationships were used for the alluvial fill and rockfill materials in the dam, and the Seed and Idriss (1970) sand relationships were used for the core. To account for the dependency of such relationships on effective stress, the upper bound modulus reduction relationships, and the corresponding damping relationships, were used for zones in the dam with mean effective stresses higher than 10 tsf, as outlined in Table 1.

Instrumentation

The dam site is instrumented with six 3-component strong motion accelerometers. In addition, two accelerometers are located in the river valley about 0.5 km downstream of the dam toe, at a site that may be considered representative of the free field. Other instrumentation at the dam site and on the structures includes survey monuments, inclinometers, piezometers, and flow monitoring devices.

Figure 1 shows the approximate locations of the accelerometer instruments. The center crest instruments are located near the midpoint of the crest, on the maximum dam section. The crest downhole instrument is located at a depth of 152 feet directly below the surface instrument, within the rockfill transition zone (Figure 2). The right crest instrument is located about midway between the center instrument and the right abutment. The right abutment instrument is located on rock at the crest elevation, whereas the gate chamber instrument is located at a depth of 516 feet below the crest elevation, within the left abutment. The intake tower instrument is located at the top of the structure 314 feet below the spillway crest elevation, and was damaged by submergence in 2001.

The soil conditions at the site of the downstream accelerometers consist of 37 feet of dense river alluvium underlain by about 17 feet of weathered rock, and fresh bedrock below. One instrument is located on the ground surface within a small one-story utility building, and the other at a depth of 54 feet in rock.

The accelerometers at the dam crest, right abutment, and tunnel chamber are linked to keep common timing. Similarly, the two downstream accelerometers are linked in between. However, the downstream instruments are not synchronized with the instruments at the dam site.

Reservoir Levels

The reservoir fluctuates considerably between seasons and was almost empty at the time of the Yucaipa and Big Bear Lake earthquakes. During the Yucaipa earthquake, the reservoir level was approximately 470 feet below the dam crest elevation. Water levels in the downstream alluvium fluctuate as well. The ground water level at the time of the earthquakes was estimated to be 20 feet below the ground surface at the location of the downstream accelerometers.

Recorded Seismic Response

Earthquakes

The accelerometers at the site recorded the June 16, 2005 Yucaipa, the June 12, 2005 Anza, and the February 10, 2001 Big Bear Lake earthquakes. The 2005 Yucaipa earthquake was a moment magnitude (M_w) 4.9 event located about 10 km southeast of the dam, near the Banning strand of the San Andreas Fault. Analysis of teleseismic data indicates that the earthquake was a thrust event with a focal depth of 11.8 km, most likely on a fault plane striking approximately N67ºE and dipping 62º southeast (http://www.cisn.org).

The 2001 Big Bear Lake earthquake had a magnitude M_w 5.1 and was located about 25 km northeast of the dam, whereas the 2005 Anza earthquake had a magnitude M_w 5.2 and was located about 80 km southeast of the dam. This latter event produced very small ground motions at the dam site and is not discussed further herein.

Ground Motions

The peak accelerations recorded from the Yucaipa and Big Bear Lake earthquakes are summarized in Table 2 (http://nsmp.wr.usgs.gov). The Yucaipa earthquake produced peak horizontal accelerations of about 0.2 and 0.3 g at the crest center and downstream surface instruments, respectively. The peak accelerations recorded on rock at the tunnel chamber and downstream downhole instruments were about 0.05 and 0.08 g, respectively. The peak accelerations recorded during the Big Bear Lake earthquake were considerably smaller. Because of space limitations, only the ground motions recorded at the dam site during the Yucaipa earthquake are further reviewed herein.

The time histories for the three components of acceleration recorded at the crest center and at the downstream downhole instruments are shown in Figure 3. The time histories at the crest instrument (Figure 3(a)) are indicative of the dam's seismic response whereas the time histories at the downstream downhole instrument (Figure 3(b)) are roughly representative of the free-field rock motions near the site. The time histories show that the duration of strong acceleration shaking was about 3 seconds at the crest and about 2 seconds in rock downstream. The amplitude of acceleration during strong shaking is similar for the two horizontal components at the crest, and that is also the case for the accelerations in rock downstream.

Figure 4 shows the 360º component of the acceleration time histories recorded at the crest center, right abutment, tunnel chamber, and downstream locations. That component of ground motion is nearly transverse (within a 10º angle) to the dam centerline at the location of the center crest instrument, and thus, is approximately parallel to the upstream-downstream alignment of the dam maximum section. As shown in Figure 4, there is large amplification in acceleration amplitude between the motions recorded at the crest surface and those recorded at the crest downhole instrument. Likewise, there is large amplification between the motions recorded at the downstream surface and those at the downhole instrument below. The amplification between the motions recorded at the tunnel chamber and those at the right abutment is also large. A similar degree of amplification was observed for the 90º-component accelerations.

Figure 5 shows plots of horizontal particle acceleration, velocity, and displacement for the center crest surface and downhole instruments. Analogous plots for the downstream surface and downhole instruments are shown in Figure 6. It may be seen that the downstream motions at the surface and at the downhole instrument in rock have a predominant NW-SE orientation. This orientation is consistent with the mechanism of the earthquake source and its location relative to the dam site. On the other hand, the plots of particle velocity and displacement at the center crest location have a predominant orientation slightly E-W of N-S (Figure 5). Such orientation is transverse to the dam crest at the location of the instruments and coincides with the upstream-downstream direction of the dam maximum section. The change in orientation of the ground motions between the downstream and the dam crest instruments clearly reflects vibration at the dam crest center in an upstream-downstream direction.

Vibration Characteristics

Various techniques were employed to identify the vibration characteristics of the dam. In addition to inspecting the recorded time histories, the recorded motions were examined in terms of Fourier spectral amplitudes and ratios. In addition, cross spectra were used to identify resonant frequencies of the dam, using the system identification techniques described by Bendat and Piersol (1980). All of the above techniques yielded generally consistent estimates for the first few natural frequencies of vibration of the dam. Selected spectral ratios are discussed herein.

It should be noted that the concept of modes of vibration and natural frequencies is strictly not applicable to an unbounded non-linear system such as the dam and its foundation. Nonetheless, the term 'natural frequencies' is used to denote those frequencies at which the dam motions show significant amplification with respect to selected reference motions, and in particular the downstream bedrock motions.

The Fourier spectral ratios between the crest surface and crest downhole acceleration records, and between the crest surface and the downstream downhole records are shown in Figure 7. The ratios were obtained by first smoothing the Fourier spectral amplitudes with a running 1-Hz-aperture triangular weighting function. The ratio for the 360º component between the crest surface and the downstream downhole motions suggests that the fundamental frequency of upstream-downstream vibration of the dam was about 1.2 Hz.

The two ratios for the 360º-component motions in Figure 7 show a peak at a frequency of about 3.6 Hz, possibly corresponding to a higher mode of upstream-downstream vibration. The ratios for the 90º-component motions show peaks at about 1.5 Hz and 3.5 Hz. The peak at 1.5 Hz likely represents a mode of cross-canyon vibration, whereas the peak at 3.5 Hz possibly indicates coupling with the upstream-downstream mode. A vertical mode of vibration seems apparent on the ratio for the vertical-component motions at about 2 Hz. Analogous analyses for the Big Bear Lake earthquake identified approximately the same modes of vibration of the dam (Mejia and Dawson, 2007).

Dynamic Response Analysis

Analysis Models

The seismic response of the dam during the Yucaipa and Big Bear Lake earthquakes was analyzed with 3-D and 2-D finite difference techniques using the computer program FLAC (Itasca, 2005). The analyses were used to evaluate the ability of such techniques to simulate the recorded response of the dam, and to develop a better understanding of its vibration modes.

Because the intensity of shaking at the site was relatively low, it seems unlikely that the earthquakes would have induced intense non-linear stress-strain behavior in the dense embankment materials. Accordingly, the use of equivalent-linear procedures to approximate the non-linear behavior of the embankment materials during the earthquakes was deemed suitable. Nonetheless, fully non-linear analyses were also performed using the 'hysteretic' stress-strain model available with the program FLAC (Itasca, 2005). The equivalent-linear analyses are described herein.

Because the dam is located in a relatively narrow canyon and has a curved axis, a 3-D analysis model is appropriate to understand and simulate its dynamic response. Figure 8 shows the 3-D finite element mesh of the dam and its foundation in perspective (Figure 8(a)) and in cross-section (Figure 8(b)). The mesh has about 90,000 elements and 95,000 nodes. It includes the bedrock foundation and abutments to allow for asynchronous motion on the dam foundation, and to properly represent potential interaction between the dam and its abutments.

As shown in Figure 8(a), considerable care was taken to replicate the geometry of the dam and the topography of the surrounding nearby ground. To simulate the unbounded extent of the foundation and abutments, the model is equipped with free-field boundaries on the sides and with a compliant base at the bottom. As shown in Figure 8(b), the embankment model consists of the core, upstream alluvial fill, and downstream rockfill zones. Those materials and the foundation alluvium were assumed to be saturated below the estimated location of the phreatic surface at the time of the earthquakes.

The 2-D analyses were performed with a plane strain model corresponding to a section of the 3-D model cut at the location of the dam maximum section. The 2-D model also includes the bedrock foundation and is equipped with free-field side boundaries and a compliant base.

Model Vibration Characteristics

Before using the 3-D and 2-D models to analyze the recorded response of the dam, the vibration modes of the models were examined using harmonic base excitation. Those analyses were conducted using the maximum shear moduli, G_{max}, of the embankment materials, and assuming elastic behavior with low material damping.

The models were shaken in the N-S direction with base motions corresponding to single-frequency, constant-velocity-amplitude outcrop motions. Multiple analyses were performed by varying the frequency of the input motion over a range spanning the first few modes of vibration

of the models. The variation with frequency of the ratio between the crest center motion and the input outcrop motion (i.e. the crest amplification function) was used to identify the fundamental vibration frequencies of the models. In addition, the displacement patterns at the fundamental frequencies were calculated to examine the corresponding mode shapes.

The fundamental mode of the 3-D elastic model was found to have a frequency of about 1.37 Hz with a crest amplification ratio of about 13. A second mode of upstream-downstream vibration was identified with a frequency of about 1.75 Hz. The 2-D elastic model was found to have a first mode frequency of about 1.25 Hz with an amplification ratio of about 8, and a second mode frequency of about 2.1 Hz.

Analysis for Recorded Motions

The 3-D and 2-D models were used to analyze the response of the dam during the Yucaipa and Big Bear Lake earthquakes. In addition to performing 3-D and 2-D analyses for the initial estimates of the input parameters, multiple 3-D analyses were performed to evaluate the sensitivity of the results to various assumptions, and the effects of uncertainties in the input parameters on uncertainty in the calculated dam response.

Mejia and Dawson (2006) showed that the motion on a free-field outcrop of the materials at the base of the 3-D and 2-D models of the dam is an appropriate input motion for dynamic analysis of such systems with FLAC. Because the location of the downstream accelerographs may be considered representative of the free field near the dam, those instrument records were used to derive the rock outcrop motions for input into the dam analyses. The rock outcrop motions were calculated from a one-dimensional wave propagation analysis of the seismic response of the downstream instrument site. A model of the site was developed using the known site stratigraphy and was shaken with the recorded downhole motions.

Good agreement was obtained between the calculated and recorded motions at the ground surface indicating that the selected model provides a reasonable representation of the seismic response at the downstream instrument site, and is a sensible tool for estimating the free-field outcrop rock motions. The calculated outcrop motions are very close to the recorded downhole bedrock motions, as might be expected given the limited thickness of overburden above the bedrock accelerograph.

Three-dimensional Analysis

All three components of the calculated outcrop rock motion were input simultaneously in the 3-D dynamic response analyses. In addition, analyses were also performed for the individual horizontal components of the input motions to further evaluate the amount of coupling between components of the dam motions. The timing of the input motions was adjusted to account for the difference in elevation between the base of the model and the downstream bedrock instrument, and the lack of common timing between the dam site and downstream instruments.

The analyses for the estimated dam material and foundation properties and input ground motions during the Yucaipa and Big Bear Lake earthquakes, termed the baseline case, are

presented herein. Multiple parametric analyses were performed to assess the main sources of uncertainty in the calculated dam response, and to evaluate the sensitivity of the analysis results to the input assumptions. In addition, analyses were performed using the material properties adopted in the dynamic analyses for design of the dam (USACE, 1992; Makdisi et al., 1996).

The results of the analyses for the Yucaipa earthquake are illustrated in Figures 9 to 13. As shown in Figures 9 and 10, the calculated and recorded 360º-component acceleration, velocity, and displacement time histories at the crest center and crest downhole locations, respectively, are in reasonable agreement. A similar degree of agreement was observed for the other horizontal component and less so for the vertical component. Figures 11 and 12 show analogous comparisons for the tunnel chamber and right abutment locations. Whereas the calculated and recorded time histories at the tunnel chamber agree reasonably well, the calculated and recorded histories at the right abutment are significantly different. Furthermore, there is a clear time lag between the calculated and recorded time histories. Those differences suggest significant discrepancies between the incident wave field, and/or possibly the bedrock wave propagation velocities, and the corresponding model assumptions.

Figure 13 compares the calculated and recorded spectral ratios between the 360º-component crest surface and crest downhole accelerations and between the crest surface and downstream downhole accelerations. The calculated and recorded ratios between the crest surface and downstream motions are in reasonable agreement, whereas those between the crest surface and downhole motions differ somewhat. A higher degree of agreement was observed in the ratios for the 90º component and the vertical component.

The results of the analyses for the Big Bear Lake earthquake are illustrated in Figures 14 to 16. Figures 14 and 15 show the calculated and recorded 360º-component acceleration, velocity, and displacement time histories at the crest center and crest downhole locations, respectively. It may be seen that the calculated and recorded velocities and displacements are in fair agreement whereas agreement between accelerations is limited. Figure 16 compares the calculated and recorded spectral ratios between the crest surface and crest downhole motions, and between the crest surface and downstream downhole motions. There is reasonable agreement between the calculated and recorded crest surface/crest downhole ratios, whereas the crest surface/downstream downhole ratios differ significantly.

Two-dimensional Analysis

Analyses were performed using the 2-D FLAC model of the dam maximum section for comparison with the results of the 3-D analyses. The analyses were performed using the same equivalent-linear methodology and material properties as those used in the 3-D analyses. The input motions were also the same as in the 3-D analyses, except that only the 360º and vertical components were used.

The results of the 2-D analysis for the Yucaipa earthquake are shown in Figures 17, 18 and 13. Figure 17 compares the 360º-component time histories calculated at the crest surface from the 2-D and 3-D analyses with the recorded time histories. Figure 18 shows an analogous comparison for the time histories calculated at the crest downhole instrument. It may be seen

that the motions calculated from the 2-D analysis are similar to those calculated from the 3-D analysis. This is also the case for the calculated spectral ratio between the crest surface and crest downhole motions, and less so for the ratio between the crest surface and downstream downhole motions, as shown in Figure 13.

Discussion

The results of the analyses indicate that available 3-D analysis procedures are capable of simulating the recorded response of the dam during the Yucaipa and Big Bear Lake earthquakes reasonably well. Although reasonable agreement was obtained between the calculated and recorded time histories at the crest and corresponding spectral ratios, the results suggest that considerable uncertainties are associated with the assumed analysis inputs. The main sources of uncertainty appear to lie in the nature of the seismic wave field at the site and the properties of the embankment materials. Significant uncertainty also seems associated with the properties of the dam foundation. Parametric analyses suggest, however, that the calculated horizontal dam response is not highly sensitive to reasonable assumptions for the shear wave velocity of the foundation rock.

The observed difference in the fundamental frequency of vibration during the Yucaipa earthquake indicates that the overall stiffness of the dam is slightly lower than that in the 3-D model. On the other hand, the difference in amplification frequencies between the crest surface and crest downhole motions indicate that the stiffness of the upper 150 feet of the dam is somewhat higher than in the model. Such differences are likely associated with the assumptions for the K_{2max} values and modulus reduction relationships of the embankment materials, and possibly the assumption for the values of Poisson's ratio. The uncertainties in K_{2max} values would be considerably reduced through measurements of the shear and compression wave velocities of the embankment materials in place.

The results of the analyses indicate that the materials likely exhibited significant nonlinear behavior in spite of the moderate intensity of shaking during the Yucaipa earthquake. The analyses results suggest that shear strains throughout the dam exceeded 10^{-3}% and approached 10^{-2}% near the crest, and highlight the importance of the embankment modulus reduction and damping relationships in simulating the dam response.

The good agreement between the crest time histories and spectral ratios calculated with the 3-D and 2-D analyses models suggest that 3-D behavior may not have played as significant a role as anticipated in the upstream-downstream seismic response of the dam maximum section. This may be due to the fact that the canyon has a trapezoidal shape and the average dam height above the base of the canyon is about 550 feet, which yields a crest length to height ratio of about 5, near the threshold value for significant 3-D effects.

Summary and Conclusions

The recorded response of Seven Oaks Dam during the 2005 Yucaipa and the 2001 Big Bear Lake earthquakes was analyzed to identify the dam's key response characteristics. The seismic response of the dam during the earthquakes was analyzed with 3-D and 2-D finite

difference procedures using detailed geometric models of the dam and its foundation. The dynamic material properties were estimated based on field and laboratory data obtained prior to construction. Multiple analyses were also performed to evaluate the sensitivity of the results to various model assumptions and the effects of uncertainties in the input parameters on the calculated dam response.

The results of the analyses indicate that available 3-D analysis procedures are capable of simulating the recorded response of the dam during the Yucaipa and Big Bear Lake earthquakes reasonably well. However, the results suggest that considerable uncertainties are associated with the assumed analysis inputs. The main sources of uncertainty appear to lie in the assumed seismic wave field at the site, and the properties of the embankment materials. The uncertainties in the shear moduli of the embankment materials at small strains would be considerably reduced through in-situ measurements of the shear and compression wave velocities of the embankment materials.

The results of the analyses indicate that the embankment materials likely exhibited significant nonlinear behavior during the Yucaipa earthquake. Thus, the modulus reduction and damping relationships for the embankment materials are key parameters required to adequately simulate the dam response during the earthquake.

Good agreement was obtained in the calculated crest acceleration response of the dam maximum section with 3-D and 2-D analysis procedures. Thus, the analyses results suggest that 3-D behavior may not have played a major role in the recorded upstream-downstream response at the dam crest center.

Acknowledgements

References

Bendat, J.S. and Piersol, A.G. (1980). Engineering applications of correlation and spectral analysis, John Wiley and Sons.

Boulanger, R.W., Bray, J.D., Merry, S.M., and Mejia, L.H. (1995). "Three-dimensional dynamic response analyses of Cogswell dam." Canadian Geotechnical Journal, 32(3), 452-464.

Dakoulas, P. (1993). Earth dam-canyon interaction effects for obliquity incident SH waves," Journal of Geotechnical and Geoenvironmental Engineering, ASCE, 119(11), 1696-1716.

Hardin, B.O., and Kalinski, M.E.. (2005). "Estimating the shear modulus of gravelly soils," Journal of Geotechnical and Geoenvironmental Engineering, ASCE, 131(7), 867-875.

Itasca (2005) *FLAC, Fast Lagrangian Analysis of Continua, User's Guide*. Minneapolis, Minnesota, USA.

Makdisi, F.I., Roodsari, A.T., Madianos, M.N. and Wang, Z.-L. (1996). "Evaluation of Seismic Stability of Seven Oaks Dam," Sixteenth Annual USCOLD Lecture Series, Los Angeles, California, July 22-26.

Mejia, L.H. and Seed, H.B. (1983). "Comparison of 2-D and 3-D dynamic analyses of earth dams," Journal of the Soil Mechanics and Foundation Division, ASCE, 109, GT11, 1383-1398.

Mejia, L.H., Sykora, D.W., Hynes, M.E., Fung, K., Koester, J. (1991). "Measured and calculated dynamic response of rockfill dam," Proceedings, 2nd International Conference on Recent Advances in Geotechnical Earthquake Engineering and Soil Dynamics, March, St. Louis, Mo., 1063-1070.

Mejia, L.H., and Dawson, E.M. (2006). "Earthquake deconvolution for FLAC," Proceedings, Fourth International FLAC Symposium on Numerical Modeling in Geomechanics, Madrid, Spain, May.

Mejia, L.H., and Dawson, E.M. (2007). "Analysis of seismic response of Seven Oaks Dam," Report prepared for the California Geological Survey, Strong Motion Instrumentation Program (SMIP), URS Corporation, Oakland, California.

Rollins, K.M., Evans, M.D., Diehl, N.B., and Daily, W.D. (1998). "Shear modulus and damping relationships for gravels," Journal of Geotechnical and Geoenvironmental Engineering, ASCE, 124(5), 396-405.

Seed, H.B. and Idriss, I.M. (1970). "Soil moduli and damping factors for dynamic response analysis," Report No. EERC 70-10, University of California, Berkeley, Earthquake Engineering Research Center.

Seed, H.B., Wong, R.T., Idriss, I.M. and Tokimatsu, K. (1986). "Moduli and damping factors for dynamic analyses of cohesionless soils," Journal of Geotechnical and Geoenvironmental Engineering, ASCE, 112(11), 1016-1032.

U.S. Army Corps of Engineers (USACE). (1992). "Design Memorandum No. 8, Feature Design – Seven Oaks Dam, Embankment and Spillway, Volume 2 – Appendix A, Dynamic Analysis Supplement," Report prepared by the USACE, Los Angeles District, December.

Table 1. Properties for Dynamic Analysis of Seven Oaks Dam

Material	Moist Unit Weight (lbs/ft^3)	Saturated Unit Weight (lbs/ft^3)	K_{2max}	Poisson's Ratio[1]	Modulus Reduction	Damping
Core	136	138	70	0.45 (0.48)	S&I Sands Ave[2]	S&I Sands ALB[3]
Rockfill	142	148	160	0.33 (0.45)	Seed et al Gravels Ave[4]	Seed et al Gravels Ave
Alluvial Fill	146	149	175	0.33 (0.45)	Seed et al Gravels Ave	Seed et al Gravels Ave
Foundation Alluvium	146	149	275	0.33 (0.45)	Seed et al Gravels Ave	Seed et al Gravels Ave
Weathered Rock[5]	165	170	$V_s = 3000$ ft/sec	0.33 (0.4)	Idriss W. Rock[6]	Idriss W. Rock
Bedrock	170	170	$V_s = 6000$ ft/sec	0.33 (0.33)	Elastic	0.5%

Notes: [1] Values of Poisson's ratio in parenthesis are for saturated materials.
   [2] Average relationship for sands by Seed and Idriss (1970). For effective mean stresses greater than 10 tsf, the upper bound relationship was used.
   [3] Intermediate between the average and lower bound curves by Seed and Idriss (1970). For effective mean stresses greater than 10 tsf, the lower bound relationship was used.
   [4] Average relationship for gravels by Seed et al. (1986). For effective mean stresses greater than 10 tsf, the upper bound modulus reduction and intermediate lower bound damping relationships were used.
   [5] For analysis of downstream free-field motions.
   [6] Average relationship for weathered rock by Idriss (personal communication).

Table 2. Peak accelerations recorded at Seven Oaks Dam Site (g's)

Instrument	2005 Yucaipa Eq.			2001 Big Bear Lake Eq.		
	360°	90°	UP	360°	90°	UP
Center crest Surface	0.196	0.188	0.110	0.026	0.029	0.025
Center crest downhole	0.086	0.078	0.036	0.014	0.017	0.018
Right crest	NA	NA	0.110	0.029	0.025	0.011
Right abutment	0.208	0.127	0.095	0.011	0.011	0.009
Tunnel chamber	0.054	0.045	0.027	0.005	0.007	0.004
Downstream surface	0.290	0.224	0.173	0.041	0.060	0.017
Downstream downhole	0.075	0.079	0.038	0.007	0.020	0.006
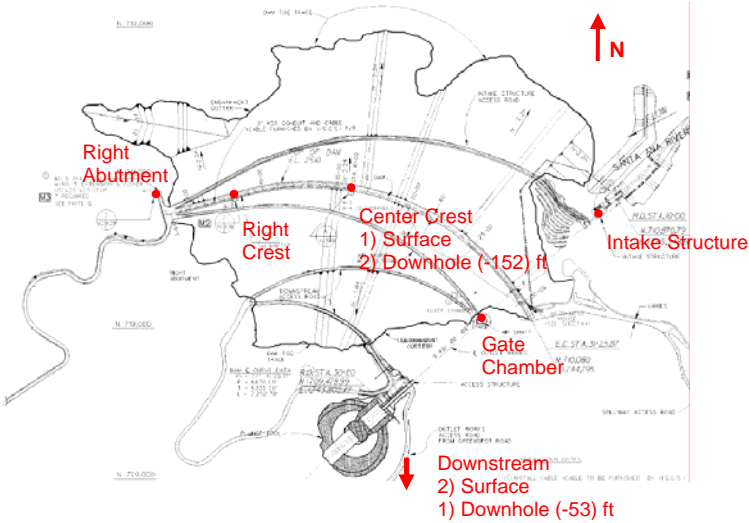
Figure 1. Plan view of Seven Oaks Dam showing accelerographs locations
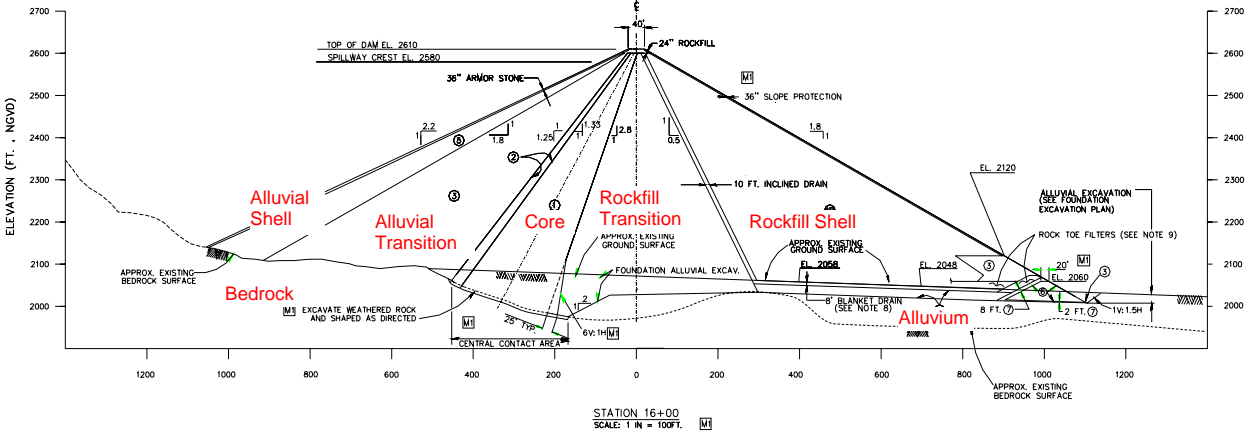
Figure 2. Maximum cross section of Seven Oaks Dam

a) Crest Surface   b) Downstream Downhole
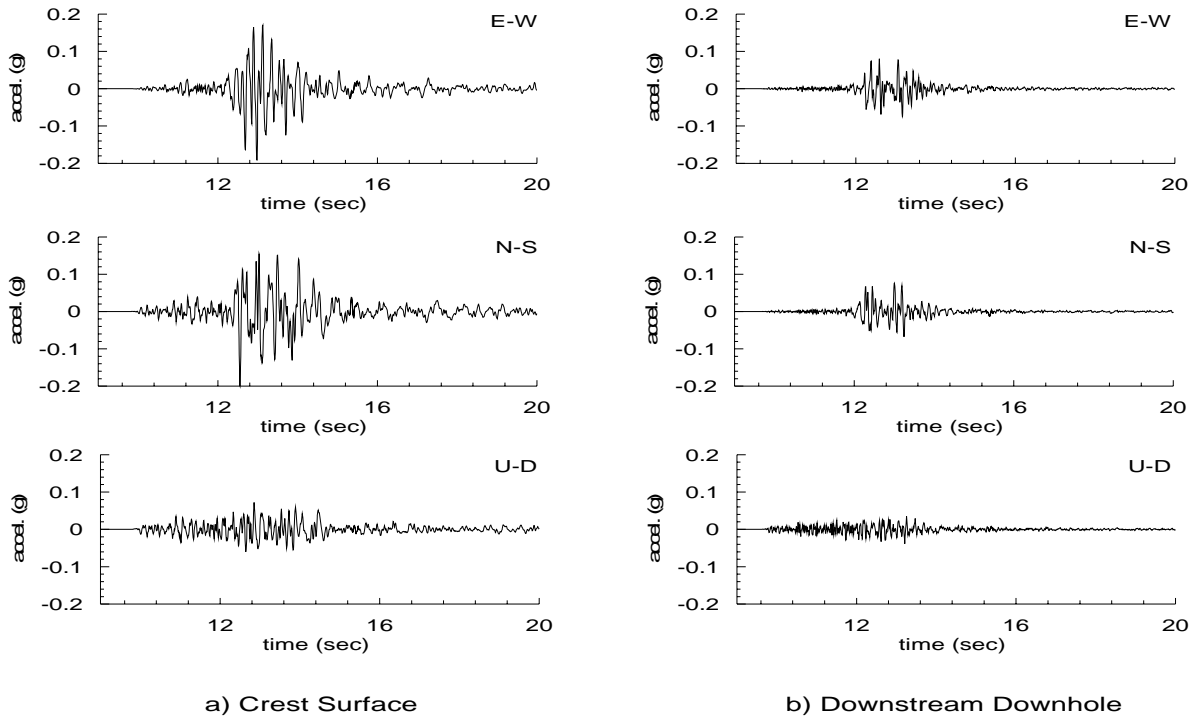
Figure 3. Acceleration time histories recorded at dam crest and downstream
downhole instruments during the Yucaipa earthquake
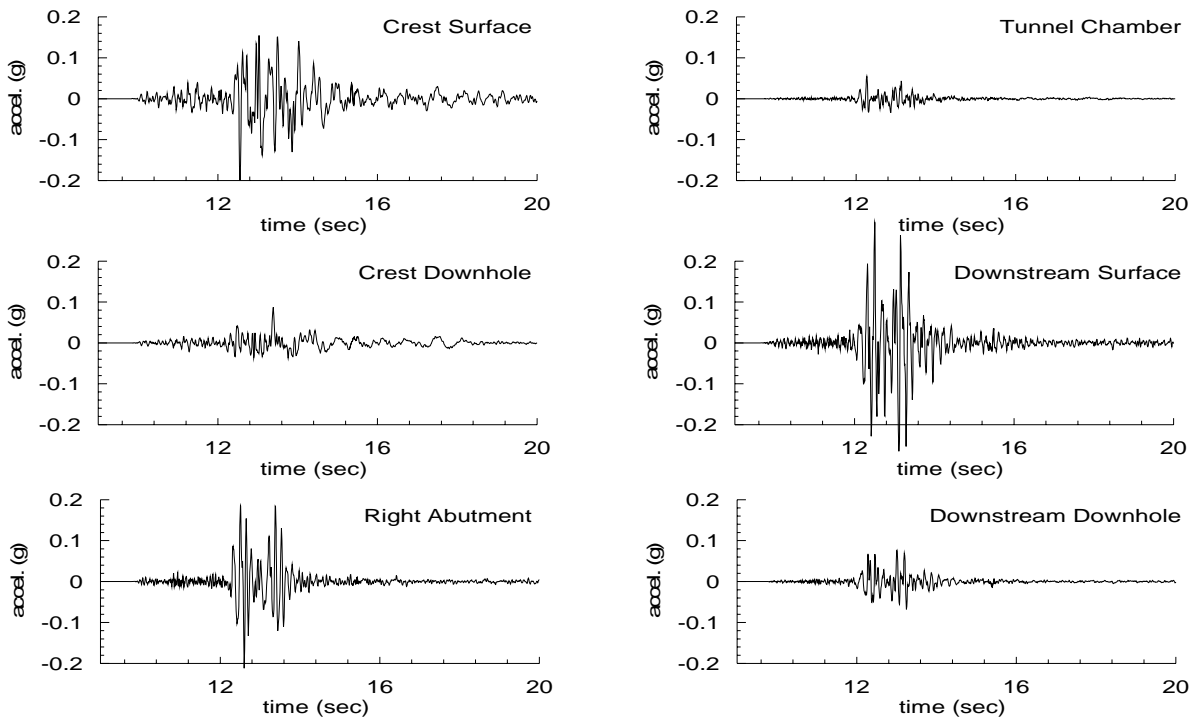
Figure 4. North-south acceleration time histories recorded at selected dam-site
and downstream locations during the Yucaipa earthquake
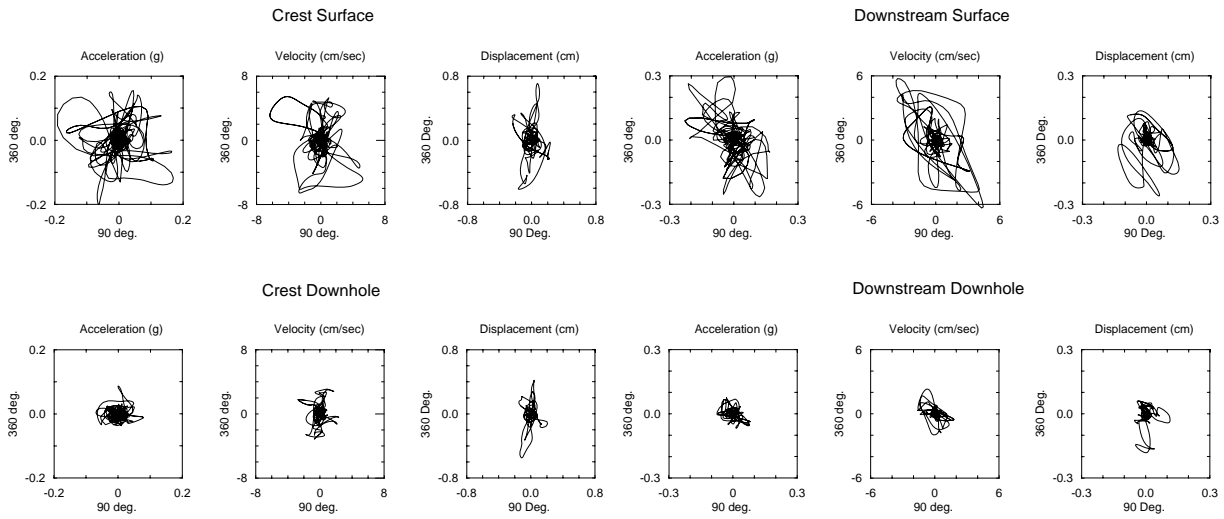
Figure 5. Horizontal particle acceleration, velocity and displacement at the crest surface and downhole instruments during the Yucaipa earthquake

Figure 6. Horizontal particle acceleration, velocity and displacement at the downstream surface and downhole instruments during the Yucaipa earthquake
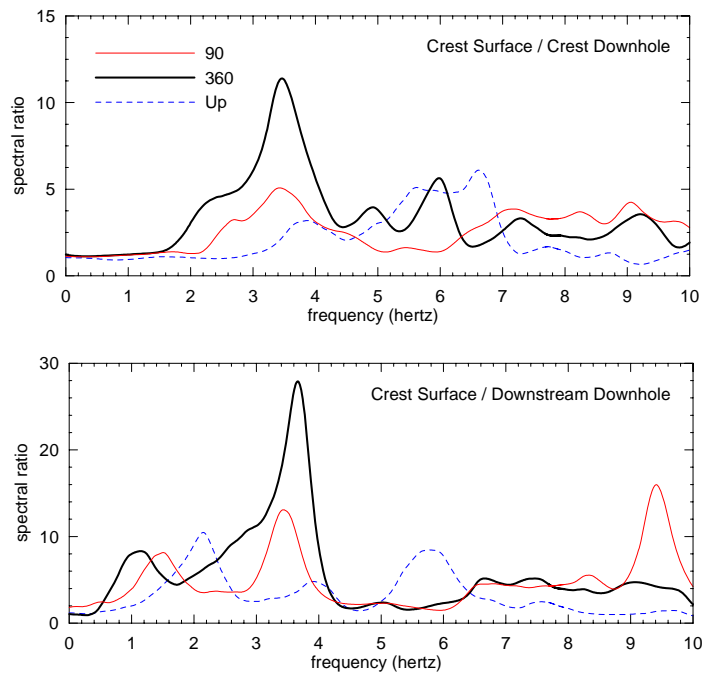
Figure 7. Fourier spectral ratios between selected acceleration records from the Yucaipa earthquake

a) Perspective View

Upstream (north)

Downstream (south)

alluvium
rockfill
rock_transition
core
bedrock
alluvial_transition

b) Cross-section at crest midpoint
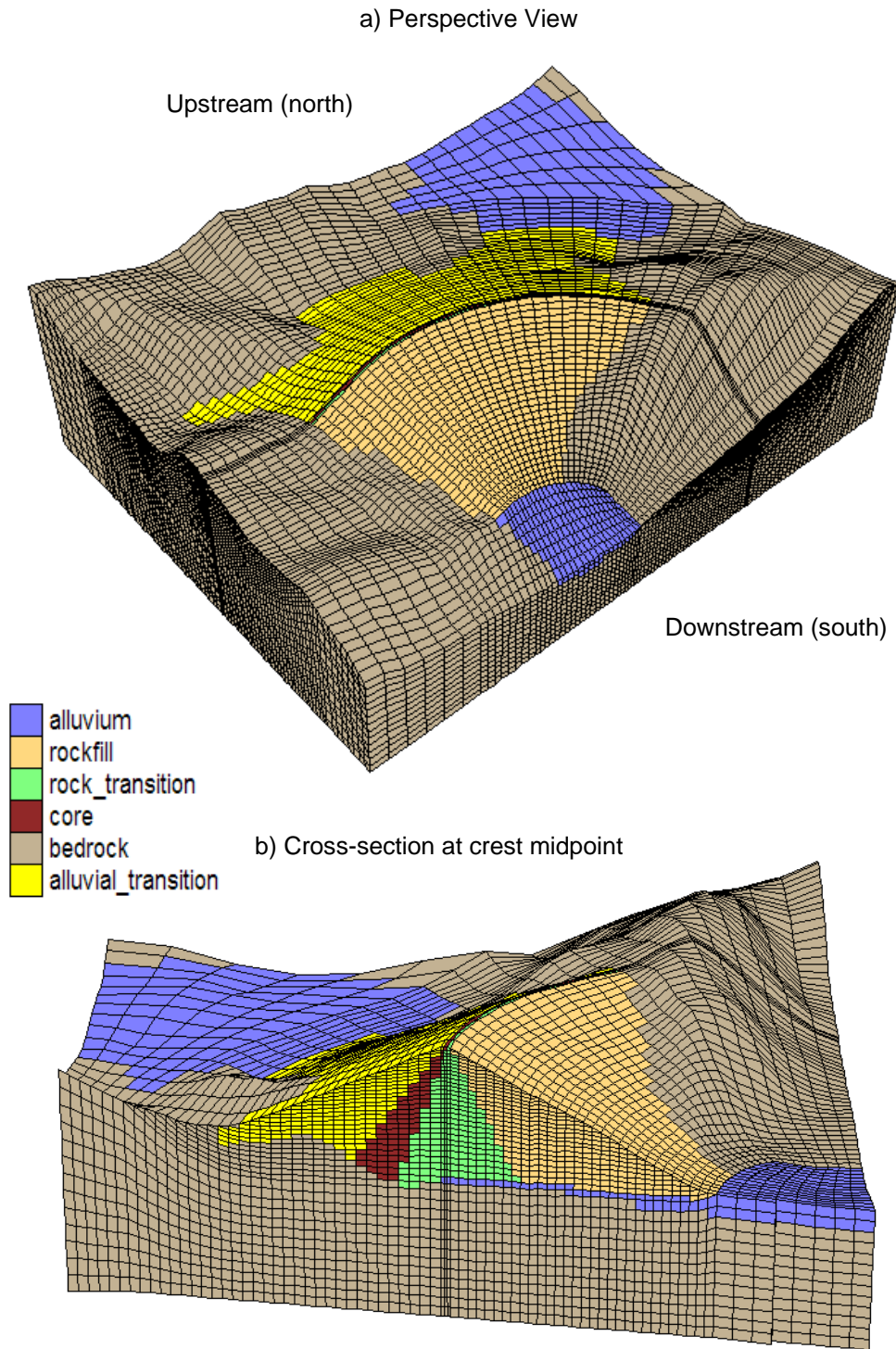
Figure 8. Three-dimensional finite element mesh of dam
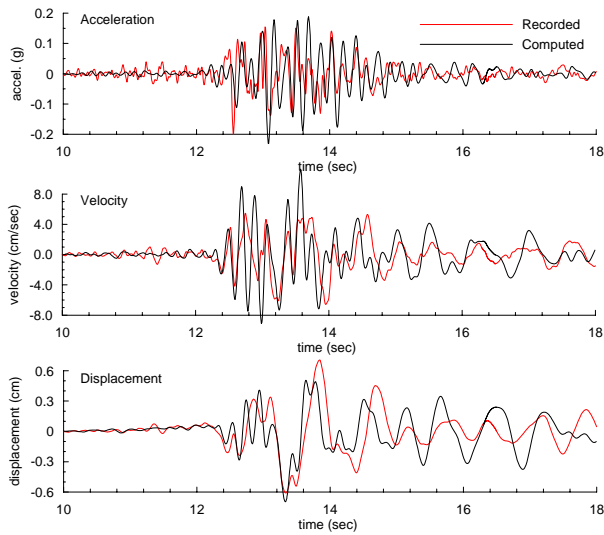
Figure 9. Calculated and recorded N-S time histories at crest surface for the Yucaipa earthquake – 3-D analysis
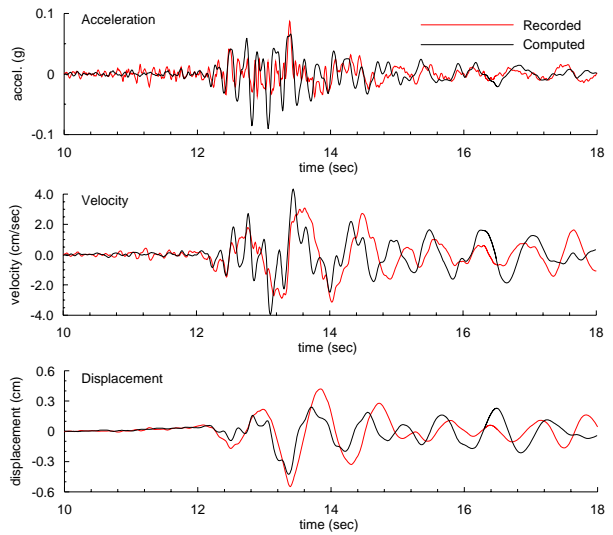
Figure 10. Calculated and recorded time histories at the crest downhole instrument for the Yucaipa earthquake – 3-D analysis
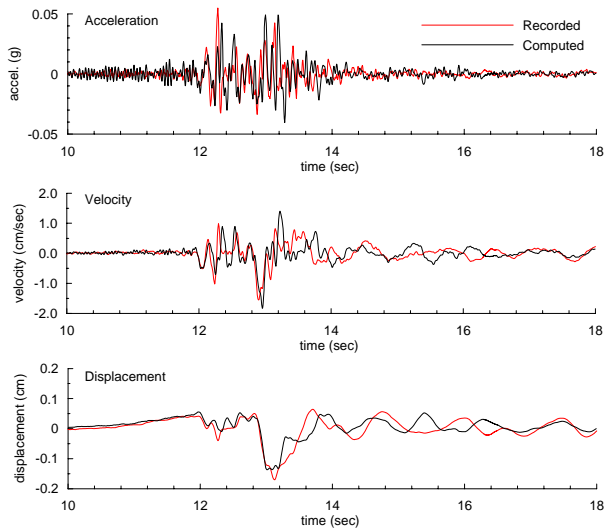
Figure 11. Calculated and recorded N-S time histories at the tunnel chamber for the Yucaipa earthquake – 3-D analysis
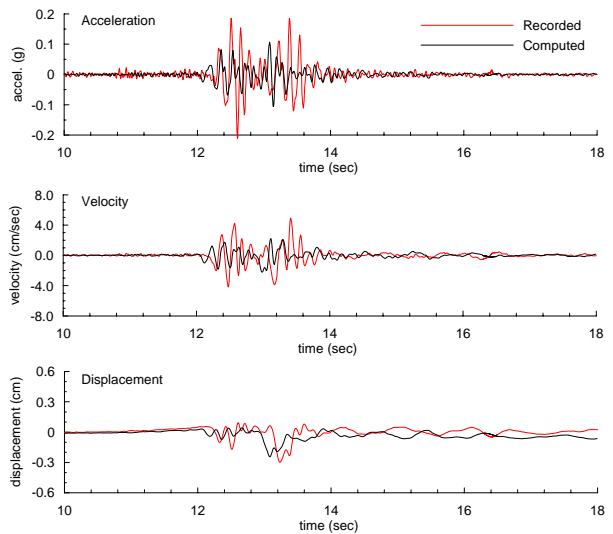
Figure 12. Calculated and recorded N-S time histories at the right abutment for the Yucaipa earthquake – 3-D analysis
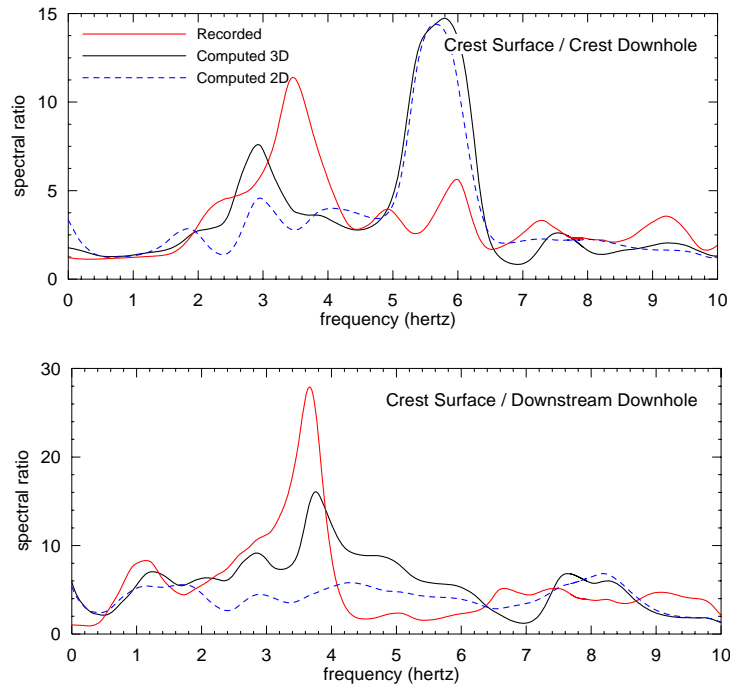
Figure 13. Comparison of N-S spectral ratios calculated from 3-D and 2-D analyses for the Yucaipa earthquake with recorded ratios
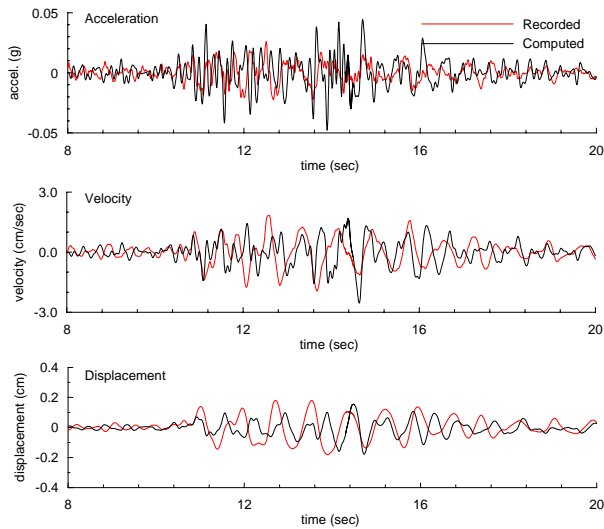
Figure 14. Calculated and recorded time histories at the crest surface for the Big Bear Lake earthquake – 3-D analysis
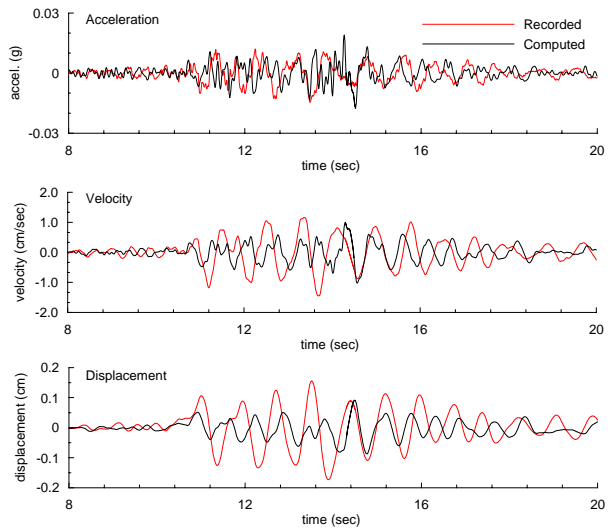
Figure 15. Calculated and recorded time histories at the crest downhole instrument - Big Bear Lake earthquake – 3-D analysis
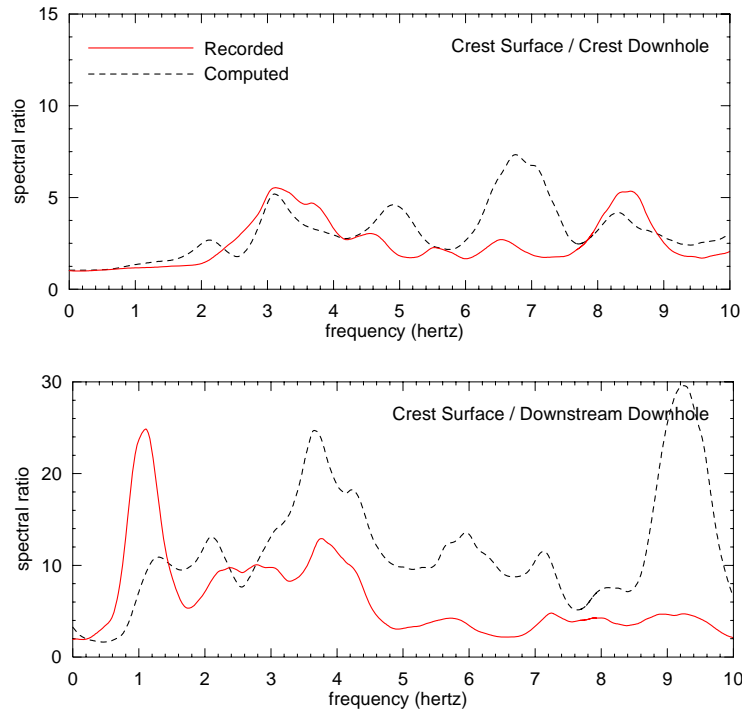
Figure 16. Calculated and recorded N-S acceleration Fourier spectral ratios for the Big Bear Lake earthquake – 3-D analysis
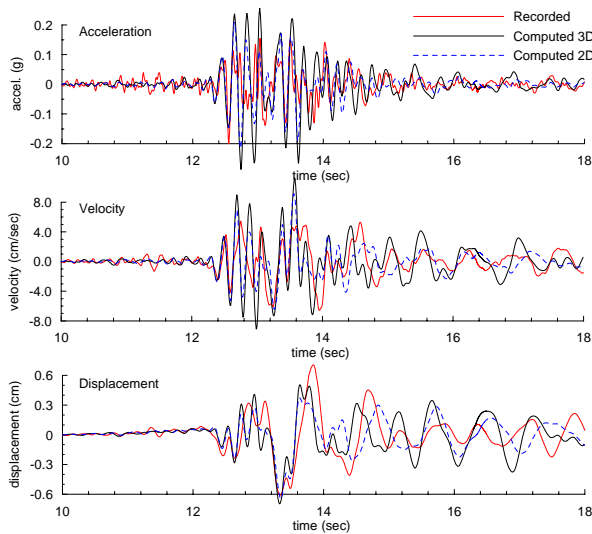
Figure 17. Comparison of N-S motions calculated at the crest surface from 2-D and 3-D analyses with recorded motions – Yucaipa earthquake
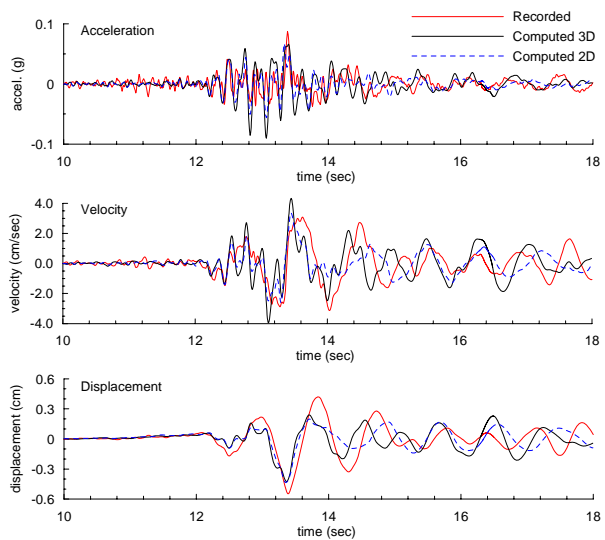
Figure 18. Comparison of N-S motions calculated at the crest downhole from 2-D and 3-D analyses with recorded motions – Yucaipa earthquake